Simple Model for the Mechanics of Spider Webs

Yuko Aoyanagi and Ko Okumura*
Department of Physics, Ochanomizu University, 2-1-1, Otsuka, Bunkyo-ku, Tokyo 112-8610, Japan
(Received 22 September 2009; published 20 January 2010)

We propose a simple model to describe spider orb webs. The model has a formal analytical solution when no thread elements are broken. When the radial threads are sufficiently strong compared to the spiral threads, the model is free of stress concentrations even when a few spiral threads are broken. This is in contrast with what occurs in common elastic materials. According to our model, spiders can increase the number of spiral threads to make a dense web (to catch small insects) or adjust the number of radial threads (to adapt to environmental conditions or reduce the cost of making the web) without reducing the damage tolerance of the web.

DOI: 10.1103/PhysRevLett.104.038102 PACS numbers: 87.85.gp, 46.50.+a, 46.70.Lk, 62.20.mm

Although the orb web of a spider is a lightweight structure [1], it seems to be a highly optimized structure, presumably as a result of evolution from the Jurassic period or earlier [2]; it seems to resist different loads such as wind and insect impact efficiently and can catch prey even if some threads are broken. There are many studies on spider silk as a high-performance polymeric fiber, e.g., in terms of entropic elasticity [3], water coating [4], breaking strength [5], gene family [6], various structural features such as liquid-crystalline [7], micellar [8], and hierarchical [9] structures, and torsional relaxation [10]. However, very little is known of the structural mechanical properties of spider webs although there are a few studies on vibration [11,12], tensile prestress [13], and detailed finite-element modeling [12,14]. Here, we propose a model for the orb web, which is simple enough to allow an analytical solution. The model highlights the mechanical adaptability of the web, providing simple but comprehensible physical understanding of its static properties. We stress in this study the importance of the maximum force appearing in the system as a crucial factor for the web's toughness (or damage tolerance) when the web is subject to an extra stress due to wind or prey impact. This is because materials are commonly weakened by a strong force appearing at a fracture tip, i.e., a stress concentration [15]. In this Letter, we concentrate on orb webs although there are many varieties of web [16]. This is because the orb web is the most familiar form and presents universal structural features that are conserved across species, which suggests that it has benefited from natural selection to become adaptable.

We consider a two-dimensional (2D) orb web consisting of N radial threads and M spiral threads. The nodes where threads are linked are labeled by a set (n, m) as in Fig. 1 and their position is denoted by a 2D vector $\mathbf{X}_{n,m}$ where $n = 0, 1, 2, \ldots, N-1$ and $m = 1, 2, \ldots, M$, where $\mathbf{X}_{n,0} = (0, 0)$ (independent of n). The (n, m) element of the radial and spiral threads connects two adjacent nodes $\mathbf{X}_{n,m}$ and $\mathbf{X}_{n,m-1}$ and another set of adjacent nodes $\mathbf{X}_{n,m}$ and $\mathbf{X}_{n-1,m}$, respectively. The natural length of all (n, m) radial threads is equal to L while that of the (n, m) spiral thread l_m depends on m because of geometrical restrictions:

$$l_m = \alpha m L \equiv 2mL \sin(\pi/N). \tag{1}$$

In other words, without any tension the node positions are given in (θ, r) coordinates by

$$\mathbf{X}_{n,m} = (2n\pi/N, mL). \tag{2}$$

The spring constant of the radial thread is independent of the element and denoted $\bar{K} = K/L$ while that of the spiral thread depends on the m label and is denoted $\bar{k}_m = k/l_m$ since the spring constant is inversely proportional to the natural length. Since radial threads are stronger than spiral ones [14] we are mainly interested in the case where $K > k$. In addition, we define $F_{n,m}$ and $f_{n,m}$ as the magnitude of the force acting on the (n, m) radial and spiral threads, respectively.

It is known that an orb web is under tension when completed by a spider [13]. To mimic this situation, we expand the model web introduced as above from the original unstretched state to a homogeneously stretched state by setting the r coordinate of the peripheral node $\mathbf{X}_{n,M}$ to $ML + \Delta$ (independent of n). We regard this state as a real spider web (under tension) without any damage (we cut

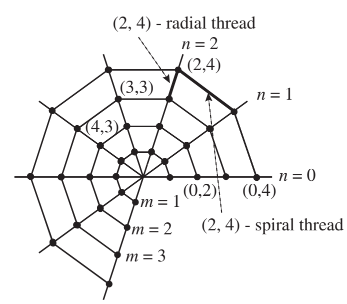

FIG. 1. Model of orb web of spider consisting of 10 radial threads and 4 spiral threads ($N = 10$, $M = 4$), which are labeled as above. See the details in the text.

some of the springs below to simulate damage). In such a state, both $F_{n,m}$ and $f_{n,m}$ are dependent not on n but on m as made clear from a symmetry argument. They are denoted F_m and f_m, respectively, and in addition satisfy the relations

$$\frac{F_{m+1}}{\bar{k}_{m+1}} = \left(\frac{1}{\bar{k}_{m+1}} + \frac{1}{\bar{k}_m} + \frac{\alpha^2}{K}\right)F_m - \frac{F_{m-1}}{\bar{k}_m} \tag{3}$$

$$F_{m+1} = F_m + \alpha f_m \tag{4}$$

with the initial conditions

$$F_1 = \bar{K}\Delta L, \qquad f_1 = \alpha \bar{k}_1 \Delta L. \tag{5}$$

Here, ΔL is the elongation of the first radial thread attached to the node $\mathbf{X}_{n,1}$. The recurrence relation in Eq. (3) between three adjacent terms can be solved formally by using a continued fraction [17]. Exact numerical estimation of the continued fraction in this case requires only a simple numerical iteration calculated in a second on a personal computer (PC) although a number of calculation schemes have been developed in general cases.

To study the static state of the web with damage, we developed a numerical code to calculate the static state of the present web model by extending the code used in [18] because the numerical iteration of Eqs. (3) and (4), with an appropriate condition describing the damage, does not work unless we allow the approximation of the fixed node points; we solved the equation of motion $d\mathbf{X}_{n,m}/dt = -\eta \mathbf{F}_{n,m}$ to seek the equilibrium state where $\mathbf{F}_{n,m}$ is the total force acting on the node $\mathbf{X}_{n,m}$ from the four springs attached to the node (see details in [18]), where the calculation is completed in around 10 min on a PC.

The typical values of the diameter, elastic modulus, and the initial tension of radial spider silks are of the order of 1 μm, 1 GPa, and 0.1 mN [14], respectively, which implies an initial strain about 0.1 and $\bar{K}$ about 1 N/m if L is about 1 mm. Our numerical results can be interpreted as, for example, the case where $\bar{K} = 1$ N/m, $L = 1$ mm, $\Delta =$ 1 mm [a characteristic strain $\varepsilon = \Delta/(ML + \Delta)$ is $1/(M + 1)$] and the unit of the force $\bar{K}\Delta = 1$ mN, while the case with a smaller strain can be obtained, e.g., simply by putting that $\Delta = 0.1$ mm and $\bar{K}\Delta = 0.1$ mN [in numerical calculations we set $\bar{K} = L = \Delta = 1$, which implies that the characteristic force $\bar{K}\varepsilon L$ is $1/(M + 1)$ in the unit of $\bar{K}\Delta = 1$]. The numbers of radial and spiral threads of the web are $N = 10$ and $M = 9$ in the numerical results given below, if they are not specified explicitly. Typical values of K and k can be given as the elastic modulus multiplied by the thread's section area: $K = 31.5$ mN and $k = 2.26$ mN from Table 1 in [14], which implies that K/k is 14 (of the order of 10). One structural reason for this high ratio is that radial threads are thicker than spiral ones although differences in chemical composition and in microscopic structure are also important [14].

The results of the force distribution in an undamaged web are shown in Fig. 2, where two cases with different

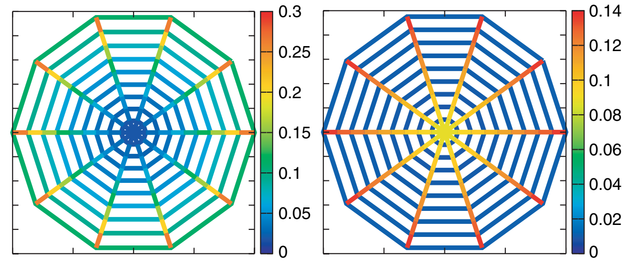

FIG. 2 (color online). Force distribution for undamaged webs (left) for $K/k = 1$ and (right) for $K/k = 10$. The right-hand plot corresponds to natural spider webs. Note that the maxima of the color scale are different in the two plots where the values are given in $\bar{K}\Delta$.

K/k ratio are compared. The threads with the maximum force are the radial threads located at the outermost positions. This is understood from Eq. (4): by iteration of this equation we see that F_{m+1} is given as the summation of $F_1, F_2, \ldots, F_m$ and $f_1, f_2, \ldots, f_m$ with positive coefficients. Physically speaking, forces on thread elements are accumulated towards peripheral radial threads in this model. In addition, we see in Fig. 2 that by making the ratio K/k larger, as in the actual spider web, we can reduce the maximum force appearing in the web. This can again be understood physically; for example, if we consider the limit where no spiral threads are present, the force accumulation from f_1, $f_2, \ldots, f_m$ is suppressed so that we expect a weaker force on the radial threads.

The above force distribution is quantified more explicitly in the left-hand plot in Fig. 3 where we have plotted the maximum force F_0 appearing in the system (or acting on the outermost radial spring) as a function of the ratio K/k. It is interesting that the maximum force drops sharply to an asymptotic value with the ratio and it almost reaches the asymptotic value when the ratio K/k is about 10, which is a typical value for real spider webs as mentioned above.

The dependence of the maximum force F_0 on the number of radial threads N in a web made up of 9 spiral threads is shown in the middle plot in Fig. 3 for two values of K/k. We see that a spider can reduce the maximum force by increasing N. However, this tendency is less when K/k reaches a typical value (around 10) for real spiders' webs. As a result, a spider can select the number of radial threads

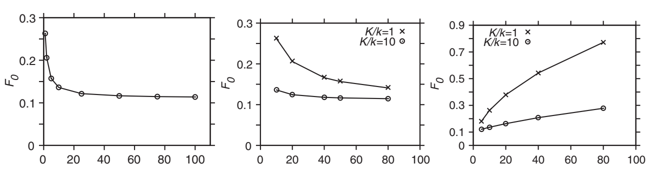

FIG. 3. The maximum force F_0 (in $\bar{K}\Delta$) appearing in the system as a function of the ratio K/k where $N = 10$ and $M = 9$ (left), as a function of the number of radial threads N for two values of K/k where $M = 9$ (middle), and as a function of the number of spiral threads M for two values of K/k where $N = 10$ (right).

N without reducing the strength of the web (i.e., with the maximum force appearing in the web changed only slightly). This is a preferable property if we consider the work of making the web for a spider and the adaptability of a spider to make the web in various environments.

The dependence of the maximum force F_0 on the number of spiral threads M is shown in the right-hand plot in Fig. 3 for two values of K/k. Here, the size of the web is fixed to the same by setting $\mathbf{X}_{n,M}$ to $9L + \Delta$ and by adjusting the radial spacing between the adjacent nodes. We see that the maximum force increases with M. However, this tendency is less when K/k reaches a typical value (around 10) for real spiders' webs; this property is an advantage for a spider that wishes to make the web denser to catch smaller insects.

We discuss below the force distribution in the spider web when one of the spiral threads is damaged (the stronger radial threads are at less risk of damage). Specifically, we compare the cases when either (2, 5) or (2, 8) spiral thread is absent. In the top panel of Fig. 4 we compare the force distribution when the spiral thread in the middle [i.e., (2, 5) spiral thread] is absent for three different values of K/k where radial and spiral threads loaded with the maximal force are indicated by arrows (the shorter arrows for the spiral thread point to the spiral threads with the second maximal force). We here find that the position of the thread with the maximum force changes with K/k. This is completely different from usual elastic materials where the maximum stress always appears near the tip [15]. This abnormal behavior can be observed regardless of the position of the damaged thread [see, as another example, the bottom panels in Fig. 4 where the (2, 8) spiral thread is absent]. In addition, if we compare the maximum forces F_0 and f_0 in the radial and spiral threads with and without damage, as in Fig. 5, we remarkably find that the maximum forces change only slightly because of the damage. The maximum force appearing in the spider web hardly changes in spite of the damage, which is distinctly different from usual elastic materials in which a crack causes severe stress concentrations and weakens the material [15]. As a matter of fact, the overall force distribution in a damaged web for $K/k = 10$ displayed in the middle column in Fig. 4 is very similar to the case without damage for $K/k = 10$ illustrated in the right in Fig. 2. This feature of spider webs implies that we have to pay attention only to the maximum force appearing in the system in undamaged webs to discuss the strength of a web.

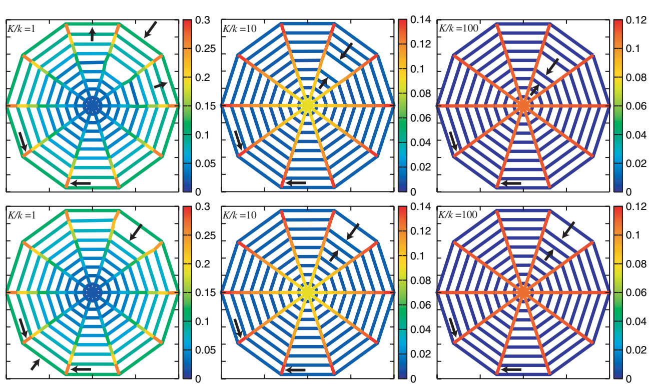

FIG. 4 (color online). The force distribution when one of the spiral threads is damaged for $K/k = 1$, 10, and 100 (from the left to the right) when a middle spiral thread (top) and an outside spiral thread (bottom) are absent. Arrows indicate the threads with the highest tension.

Other unusual features are demonstrated in Fig. 6 where we plot the force $F_{2,m}$ acting on the $(2, m)$ radial threads in the left and the force $f_{n,i}$ acting on the (n, i) spiral threads where $(2, i)$ spiral threads are absent in the right. We observe no discernible change in the radial force although the web is damaged. Furthermore, the spiral force tends to relax as a whole with showing a maximum value at a position opposite of that of the absent thread with respect to the center. These behaviors are again completely different from the usual elastic case in which a stress concentration develops near the crack.

As seen above the force distribution in our model changes little even if a spiral thread is broken. The damage tolerant behavior in this sense is understood physically if we go back to the argument developed when discussing Fig. 2. In this model forces in spiral and radial threads are accumulated towards the peripheral radial threads. However, if the spiral thread is very soft this accumulation mechanism does not work well: the web is composed mainly of the radial threads and the spiral threads play only a minor role. This is why the force distribution is unchanged if we remove any spiral thread. Accordingly, if we cut many spiral threads the web topology remains similar with no stress concentration. We confirmed this fact via direct numerical calculation. Note that, on the contrary, removal of even one of the radial threads brings about a significant change in topology of the nodes; as a matter of fact, the web is connected to the environment via frame and mooring threads whose strengths are about the same as the radial threads so that damage tolerance is guaranteed if the stronger threads, including the radial threads, are not damaged.

This mechanism of damage tolerance as a result of near absence of stress concentration offers yet another example of the significance of hierarchical effects in defining the

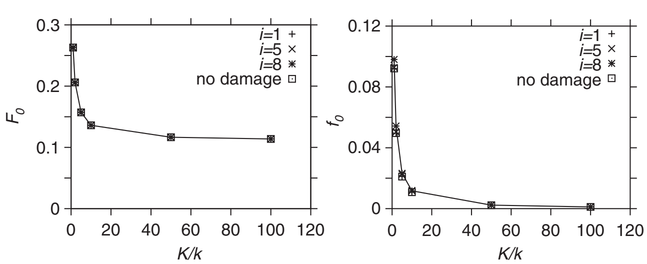

FIG. 5. The maximum forces F_0 and f_0 in the radial and spiral threads with and without damage as a function of the ratio K/k, when the $(2, i)$ spiral thread is absent where i is either 1, 5, or 8.

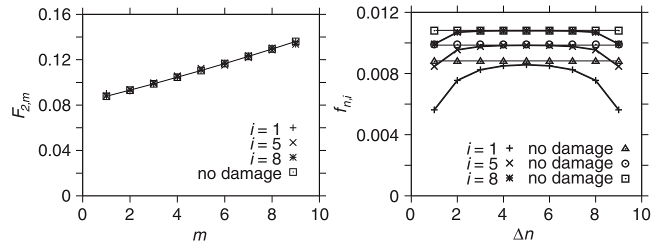

FIG. 6. Radial force $F_{2,m}$ and spiral force $f_{n,i}$ (as a function of the distance from the damaged thread, $\Delta n = n - i$) of a web with $N = 10$, $M = 9$, and $K/k = 10$, when the $(2, i)$ spiral thread is absent.

overall performance of a natural material or structure. Reduction of stress concentration in nacre has been suggested to be due to layered structures composed of soft and hard elements [19] and to the existence of nanoscale size in the hierarchical structure [20] and, on a protein network, due to mechanisms of deformation that involve mechanisms at multiple hierarchical scales (from nanoscale to macroscale) [21]. We wish to develop a multiscale model of spider webs in order to understand the hierarchical design of natural structures [20–22]. For this purpose, it is important to replace linear springs with complex springs which have different regimes of deformation of the type employed in [21]. If we replaced them with simple nonlinear springs of the type employed in a classic work [23], we expect no qualitative changes; this is because the stress concentration, which is qualitatively the same as in the linear systems, also appears in the simple nonlinear systems (or a plastic system without unloading) although the singularity is weaker [23]. This point is directly shown in simulation for a discrete network and experiment [24]. Note also that the threads in a spider's web are not springs but cables: the force acting on a thread becomes zero once it is under compression. However, we confirmed numerically that, even in cases with many spiral threads absent, almost all the springs are under tension so that the main feature remains intact if we change springs into cables.

In conclusion, we have developed a simplified model of an orb web, which allows a formal analytical solution of an undamaged spider web. We have shown that an appropriately large value of K/k (as in real spider webs) helps enhance the damage tolerance of the web, clarifying the physical origin of this remarkable feature. Furthermore, our analysis of the force distribution in a damaged spider web reveals amazing characteristics: (1) the distribution changes due to the damage but in a way quite different from ordinary elastic materials, and (2) the spider web is virtually free of stress concentrations. We expect that the physical principles found here are relevant in various contexts, e.g., in designing buildings, bridges, and space structures.

K. O. thanks MEXT, Japan for KAKENHI. We thank Fumiaki Shibata for pointing out Ref. [17] and Julian F. V. Vincent and José Bico for useful comments on our manuscript.

*okumura@phys.ocha.ac.jp

[1] P. N. Witt and C. F. Reed Science **149**, 1190 (1965).
[2] P. A. Selden, Nature (London) **340**, 711 (1989).
[3] J. M. Gosline, M. W. Denny, and M. E. DeMont, Nature (London) **309**, 551 (1984).
[4] F. Vollrath and D. T. Edmonds, Nature (London) **340**, 305 (1989).
[5] S. Osaki, Nature (London) **384**, 419 (1996).
[6] P. A. Guerette, D. G. Ginzinger, B. H. F. Weber, and J. M. Gosline, Science **272**, 112 (1996).
[7] F. Vollrath and D. P. Knight, Nature (London) **410**, 541 (2001).
[8] H.-J. Jin and D. L. Kaplan, Nature (London) **424**, 1057 (2003).
[9] H. Zhou and Y. Zhang, Phys. Rev. Lett. **94**, 028104 (2005).
[10] O. Emile, A. Le Floch, and F. Vollrath, Phys. Rev. Lett. **98**, 167402 (2007).
[11] W. M. Masters, Behav. Ecol. Sociobiol. **15**, 207 (1984).
[12] L. H. Lin, D. T. Edmonds, and F. Vollrath, Nature (London) **373**, 146 (1995).
[13] E. Wirth and F. G. Barth, J. Comp. Physiol. A **171**, 359 (1992).
[14] M. S. Alam, M. A. Wahab, and C. H. Jenkins, Mech. Mater. **39**, 145 (2007).
[15] T. L. Anderson, *Fracture Mechanics-Fundamentals and Applications* (CRC, Boca Raton, 1991).
[16] F. Vollrath and P. Selden, Annu. Rev. Ecol. Evol. Syst. **38**, 819 (2007).
[17] Risken, *The Fokker-Planck Equation* (Springer, Berlin, 1989), 2nd. ed.
[18] S. Nakagawa and K. Okumura, J. Phys. Soc. Jpn. **76**, 114801 (2007).
[19] K. Okumura and P.-G. de Gennes, Eur. Phys. J. E **4**, 121 (2001); Y. Aoyanagi and K. Okumura, Phys. Rev. E **79**, 066108 (2009).
[20] H. J. Gao, B. H. Ji, I. L. Jager, E. Artz, and P. Fratzl, Proc. Natl. Acad. Sci. U.S.A. **100**, 5597 (2003).
[21] T. Ackbarow, D. Sen, C. Thaulow, and M. Buhler, PLoS ONE **4**, e6015 (2009).
[22] M. Buhler and T. Ackbarow, Mater. Today **10**, 46 (2007).
[23] J. W. Hutchinson, J. Mech. Phys. Solids **16**, 13 (1968); J. R. Rice and G. F. J. Rosengren, J. Mech. Phys. Solids **16**, 1 (1968).
[24] Y. Aoyanagi and K. Okumura, J. Phys. Soc. Jpn. **78**, 034402 (2009); N. Sone, M. Mori, and K. Okumura (to be published).